Image Registration, Optical Flow and Local Rigidity

Martin Lefébure[1] and Laurent D. Cohen[2]

[1] Current address: 69 rue Perronet, 92200 Neuilly Sur Seine, France, was with Poseidon Technologies. Email: mlefebure@compaqnet.fr
[2] CEREMADE, Université Paris-Dauphine, 75775 Paris cedex 16, France, cohen@ceremade.dauphine.fr

Abstract. We address the theoretical problems of optical flow estimation and image registration in a multi-scale framework in any dimension. We start by showing, in the translation case, that convergence to the global minimum is made easier by applying a low pass filter to the images hence making the energy "convex enough". In order to keep convergence to the global minimum in the general case, we introduce a local rigidity hypothesis on the unknown deformation. We then deduce a new natural motion constraint equation (MCE) at each scale using the Dirichlet low pass operator. This allows us to derive sufficient conditions for convergence of a new multi-scale and iterative motion estimation/registration scheme towards a global minimum of the usual nonlinear energy instead of a local minimum as did all previous methods. We then use an implicit numerical approach. We illustrate our method on synthetic and real examples (Motion, Registration, Morphing).

1 Introduction

Registration and motion estimation are one of the most challenging problems in computer vision, having uncountable applications in various domains [13, 14, 6, 4, 10, 23]. These problems occur in many applications like medical image analysis, recognition, visual servoing, stereoscopic vision, satellite imagery or indexation. Hence they have constantly been addressed in the literature throughout the development of image processing techniques. As a first example (Figure 1) consider the problem of finding the motion in a two-dimensional images sequence. We then look for a displacement $(h_1(x_1,x_2), h_2(x_1,x_2))$ that minimizes an energy functional:

$$\int\int |I_1(x,y) - I_2(x + h_1(x,y), y + h_2(x,y))|^2 dxdy.$$

Next consider the problem of finding a rigid or non rigid deformation $(f_1(x_1,x_2), f_2(x_1,x_2))$ between two images (Figure 1), minimizing an energy functional:

$$\int\int |I_1(x,y) - I_2(f_1(x,y), f_2(x,y))|^2 dxdy.$$

Fig. 1. Two images on the left: finding the motion in a two-dimensional images sequence. Two images on the right: finding a non rigid deformation.

At last consider the stereoscopic matching problem: given a stereo pair, the epipolar constraint allows to split the two-dimensional matching problem into a series of line by line one-dimensional matching problems. One has just to find, for every line, the disparity $h(x)$ minimizing:

$$\int |I_1(x) - I_2(x + h(x))|^2 dx.$$

Although most papers deal only with motion estimation or matching depending on the application in view, both problems can be formulated the same way and be solved with the same algorithm. Thus the work we present can be applied both to registration for a pair of images to match (stereo, medical or morphing) or motion field / optical flow for a sequence of images. In this paper we will focus our attention on these problems assuming grey level conservation between both signals or images to be matched. Let us denote by $I_1(x)$ and $I_2(x)$ respectively the study and target signals or images to be matched, where $x \in D = [-M, M]^d \subset \mathbb{R}^d$, and $d \geq 1$. In the following I_1 and I_2 are supposed to belong to the space $C_0^1(D)$ of continuously differentiable functions vanishing on the domain boundary ∂D. We will then assume there exists a homeomorphism f^* of D which represents the deformation such that:

$$I_1(x) = I_2 \circ f^*(x), \forall x \in D.$$

In the context of optical flow estimation, let us denote by h^* its associated motion field defined by $h^* = f^* - Id$ on D. We thus have:

$$I_1(x) = I_2(x + h^*(x)). \tag{1}$$

h^* is obviously a global minimum of the nonlinear functional

$$E_{NL}(h) = \frac{1}{2} \int_D |I_1(x) - I_2(x + h(x))|^2 dx. \tag{2}$$

We can deduce from (1) the well known Motion Constraint Equation (also called Optical Flow Constraint):

$$I_1(x) - I_2(x) \simeq < \nabla I_2(x), h^*(x) > , \forall x \in D. \tag{3}$$

E_{NL} is classically replaced in the literature by its quadratic version substituting the integrand with the squared difference between both left and right terms of the MCE, yielding the classical energy for the optical flow problem:

$$E_L(h) = \frac{1}{2}\int_D |I_1(x) - I_2(x) - < \nabla I_2(x), h(x) > |^2 dx.$$

Here ∇ denotes the gradient operator. Since the work of Horn and Schunk [13], MCE (3) has been widely used as a first order differential model in motion estimation and registration algorithms. In order to overcome the too low spatio-temporal sampling problem which causes numerical algorithms to converge to the closest local minimum of the energy E_{NL} instead of a global one, Terzopoulos et al. [18, 23] and Adelson and Bergen [8, 22] proposed to consider it at different scales. This led to the popular coarse-to-fine minimizing technique [14, 9, 10, 19, 11]. It is based on the remark that MCE (3) is a first order expansion which is generally no longer valid with h^* searched for. The idea is then to consider signals or images at a coarse resolution and to refine iteratively the estimation process. Since then many authors pointed out convergence properties of such algorithms towards a dominant motion in the case of motion estimation [7, 9, 12], or an acceptable deformation in the case of registration [10, 19, 20], even if the initial motion were large. Let us mention that many authors assume that deformation fields have some continuity or regularity properties, leading to the addition of some particular regularizing terms to the quadratic functional [13, 5, 23, 3, 2]. This very short state-of-the-art is far from being exhaustive but it allows to raise four common features shared by all most effective differential techniques:

1. a motion constraint equation,
2. a regularity hypothesis on the deformation,
3. a multi-scale approach,
4. an iterative scheme.

However, most of the multi-scale approaches assume that the MCE is more "valid" at lower resolutions. But to our knowledge and despite the huge literature, no theoretical analysis can confirm this. It may come from the fact that blurred signals or images are always "more similar". Choosing a particular low pass operator Π_σ (here $\sigma \geq 0$ is proportional to the number of considered harmonics in the Fourier decomposition) and some deformation $f^* = Id + h^*$ satisfying a local rigidity hypothesis with respect to a signal or image I_1, we shall find a linear operator $P_\sigma^{I_1}$ depending on I_1 such that:

$$\Pi_\sigma\Big(I_1 - I_2\Big) \simeq P_\sigma^{I_1}(h^*), \tag{4}$$

the sharpness of this approximation being decreasing with respect to both h norm and resolution parameter σ. We are faced with the following motion size/structure hypothesis trade-off: for some fixed estimation reliability, the larger the motion, the poorer its structure. This transforms the problem to solving the energy minimization in a finite dimensional subspace of approximation obtained through Fourier Decomposition. In this context we are led to consider the new energy to be minimized:

$$E_L(h) = \frac{1}{2}\int_D |\Pi_\sigma(I_1 - I_2) - P_\sigma^{I_1}(h)|^2 dx.$$

Considering general linear parametric motion models for h^*, we give sufficient conditions for asymptotic convergence of the sequence of combined motion estimations towards h^* together with the numerical convergence of the sequence of deformed templates towards the target I_2. Roughly speaking, the shape of the theorem will be the following:
Theorem: If

1. at each step the residual deformation is “locally rigid”, and the associated motion can be linearly decomposed onto an “acceptable” set of functions the cardinal of which is not too large with respect to the scale,
2. the initial motion norm is not too large, and the systems conditionings do not decrease “too rapidly” when iterating,
3. the estimated deformations $Id + \hat{h}_i$ are invertible and “locally rigid”,

Then the scheme “converges” towards a global minimum of the energy E_{NL}.
The outline of the paper is as follows. In Section 2 we recall the energy convexifying properties of multi-scale approaches together with fast convergence in case of purely translational motion. In Section 3 we turn to the general motion case and introduce a new local rigidity hypothesis and a low pass filter in order to derive a new MCE of the type of equation (4). In Section 4 we design an iterative motion estimation/registration scheme based on the MCE introduced in Section 3 and prove a convergence theorem. In order to avoid the a priori motion representation problem, we adopt an implicit approach and constrain each estimated deformation to be at least invertible. We show numerical results for some signals and the stereo problem in dimension 1, and for large deformations problems in dimension 2. Section 6 gives a general conclusion to the paper.

2 Purely translational motion estimation

In this section we assume the motion to be found is only translational. This simple case will allow us to show the energy convexifying properties of multi-scale approaches together with fast convergence of iterative algorithms.

2.1 Synthetic 1D energy convexifying example

Consider a test signal (Figure 2) and its purely translated copies. The energy given by the mean quadratic error between shifted test signals and considered as a function of the translational parameter can be convexified using signals at a poorer resolution. Indeed we show the energy as a function of the translation parameter calculated with original test signals (Figure 2) and with same signal at a poorer resolution (Figure 2), namely signals reconstructed with only 5 and 3 first harmonics of the Fourier base. This readily yields more and more convexified energies as the resolution is lower. Based on this convexifying property, a generic algorithm for estimating the translational parameter is as follows:

1. Find the finest resolution j for which the energy is convex enough.
2. Minimize the MCE-based energy with signals at resolution j.
3. Refine the result by increasing the resolution and minimizing the new energy.

2.2 Convergence conditions

In [16] we prove that this iterative process can converge to the solution provided the initial motion norm is not too important with respect to the chosen signal or image resolution. This one-dimensional result was easily extended to dimension $d > 1$ (see [17]).

3 General motion multiresolution estimation

In Section 2 we have considered only purely translational motion estimation and registration. Our purpose here is to take over the general case for the motion. Our approach is based on the fact that the motion is hidden in the difference between both functions to be matched. This will lead us to analyze this difference at some particular resolution. Making some assumptions on the structure and local behaviour of the motion and the type of scale-space, we will find a new MCE and show that we can control the sharpness of it, which has not been taken care of previously.

3.1 Controlling the residuals when mixing differential and scale-space techniques

Using a regularizing kernel G_σ at scale σ, Terzopoulos et al. [18, 23] and Adelson and Bergen [8] were led to consider the following modified MCE:

$$G_\sigma * (I_1 - I_2)(x) \simeq < G_\sigma * \nabla I_2(x), h^*(x) >$$

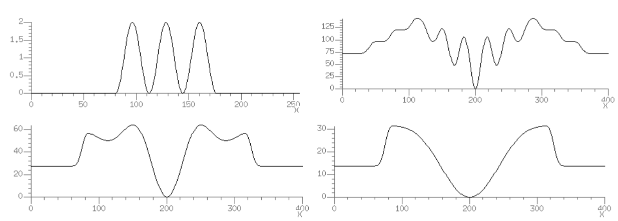

Fig. 2. Test Signal. First line: on the left, the second signal is the same shifted by 200; on the right: energy as a function of shift parameter. There are numerous local minima around the global minimum at $x = 200$ at scale 7.. Second line: same energy with signals reconstructed with only 5 harmonics (left) and 3 harmonics (right) using the multiresolution pyramid spanned by the first elements of the Fourier base.

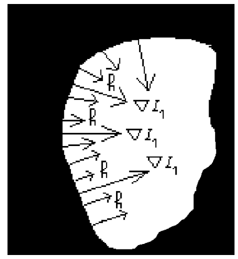

Fig. 3. An example of motion $h = f - Id$ of a ξ-rigid deformation f for image I_1. We show a level set of image I_1, and the fields ∇I_1 and h along its boundary. h varies only along the direction of ∇I_1.

To our knowledge and despite the huge literature on these approaches, no theoretical error analysis can be found when such approximations are done. However it has been reported from numerical experiments that the modified MCE was not performing well at very coarse scales, thus betraying its progressive lack of sharpness. Assuming a local rigidity hypothesis and adopting the Dirichlet operator Π_σ, we will find a different right hand side featuring a "natural" and unique linear operator $P_\sigma^{I_1}$ in the sense that:

$$\Pi_\sigma(I_1 - I_2)(x) \simeq P_\sigma^{I_1}(h^*)(x), \tag{5}$$

with remainder of the order of $\|h^*\|^2$ for some particular norm and vanishing as the scale is coarser.

3.2 Local rigidity property

In this paragraph we introduce our local rigidity property of deformations.

Definition 1. *$f \in Hom(D)$ is ξ-rigid for $I_1 \in C^1(D)$ iff:*

$$Jac(f)^t.\nabla I_1 = det(Jac(f))\nabla I_1, \tag{6}$$

where $Jac(f)$ denotes the Jacobian matrix of f and $det(A)$ the determinant of matrix A, and $Hom(D)$ the space of continuously differentiable and invertible functions from D to D (homeomorphisms).

All ξ-rigid deformations have the following properties (see [15] for the proofs). Assume f^* is ξ-rigid for $I_1 \in C_0^1(D)$ and $I_1 = I_2 \circ f^*$. Then,

1. equation (6) is always true if dimension d is 1;
2. suppose $d = 2$: then,
3. if $Jac(f^*)$ is symmetric, then (6) means that if $|\nabla I_1| \neq 0$,
   - direction $\eta = \frac{\nabla I_1}{|\nabla I_1|}$ is eigenvector ($\lambda = det(Jac(f)$ is an eigenvalue);
   - direction $\xi = \frac{\nabla I_1^\perp}{|\nabla I_1|}$ is "rigid" ($\lambda = 1$ is an eigenvalue);

   then for all $x \in D$ where I_1 is not locally constant we have $h(x) = h^*(x)$.

3.3 The Dirichlet operator

Let $D = [-M, M]^d$; $S_\sigma = \{k \in Z^d, \forall i \in [1, d], |k_i| \leq M\sigma^2\}$; $c_k(I)$ denotes the Fourier coefficient of I defined by: $c_k(I) = \frac{1}{(2M)^{\frac{d}{2}}} \int_D I(x) e^{-\frac{i\pi<k,x>}{M}} dx$. Then the Dirichlet operator Π_σ is the linear mapping associating to each function $I \in C_0^1(D)$ the function $\Pi_\sigma(I) = G_\sigma * I$, where the convolution kernel G_σ is defined by its Fourier coefficients as follows:

$$c_k(G_\sigma) = \begin{cases} 1 \text{ if } k \in S_\sigma \\ 0 \text{ elsewhere} \end{cases}$$

3.4 New MCE by Linearization for the Dirichlet projection

Now that we have introduced our rigidity property of deformations and the Dirichlet projection, we obtain the

Theorem 1. *If $f^* = Id + h^*$ is ξ-rigid for $I_1 = I_2 \circ f^* \in C_0^1(D)$, then we have:*

$$\|\Pi_\sigma(I_1 - I_2) - P_\sigma^{I_1}(h^*)\|_{L^2} \leq \frac{\pi}{2}\sigma^{d+2} \|h^* |\nabla I_1|^{\frac{1}{2}}\|_{L^2}^2.$$

This inequality is nothing but the sharpness of MCE (5): $\Pi_\sigma(I_1 - I_2)(x) \simeq P_\sigma^{I_1}(h^*)(x)$, at scale σ. It clearly expresses the fact that measuring the motion (e.g perceiving the optical flow) h^* is not relevant outside of the support of $|\nabla I_1|$.
Proof. See [17] ■

4 Theoretical iterative scheme and convergence theorem

In section 3 we found a new MCE and showed that we can control the sharpness of it. In this section we will make a rather general assumption on the motion in the sense that it should belong to some linear parametric motion model without being more specific on the model basis functions. Though it is somewhat restrictive to have motion fields in a finite dimensional functional space, this structural hypothesis will be a key to bounding the residual motion norm after registration in order to iterate the process. This makes it possible to consider a constraint on motion when there is a priori knowledge (like for rigid motion) or consider multi-scale decomposition of motion for an iterative scheme.

4.1 Linear parametric motion models and least square estimation

Let us assume the motion h^* has to be in a finite dimensional space of deformation generated by basis functions $\Psi(x) = (\psi_i(x))_{i=1..n}$. Thus h^* can be decomposed in the basis: $\exists\ \Theta^* = (\theta_i^*)_{i=1..n}$ unique, such that:

$$h^*(x) = < \Psi(x), \Theta^* > = \sum_{i=1..n} \theta_i^* \psi_i(x),\ \forall x \in Supp(|\nabla I_1|).$$

MCE (5) viewed as a linear model writes: $\Pi_\sigma(I_1 - I_2) =< P_\sigma^{I_1}(\Psi), \Theta^* >$. Now set, for σ s.t. the $P_\sigma^{I_1}(\psi_i)$ be mutually linearly independent in L^2:

$$M_\sigma = P_\sigma^{I_1}(\Psi) \otimes P_\sigma^{I_1}(\Psi), \;\; Y_\sigma = \Pi_\sigma(I_1 - I_2),$$

where $\otimes$ stands for the tensorial product in L^2. Then applying basic results from the classical theory of linear models yields: $\hat{h} =< \Psi, \hat{\Theta} >=< \Psi, M_\sigma^{-1} B_\sigma >$, where column B_σ's components are defined by $(B_\sigma)_i =< P_\sigma^{I_1}(\psi_i), Y_\sigma >$.

4.2 Estimation error and residual motion

Given the least square estimation of the motion of last paragraph, we have

Lemma 1. *In this framework the motion estimation error is bounded by inequality* $\|(\hat{h} - h^*)|\nabla I_1|^{\frac{1}{2}}\|_{L^2} \leq \frac{\pi}{2}\sigma^{d+2}\left(Tr(M_\sigma^{-1})\right)^{\frac{1}{2}} \|h^*|\nabla I_1|^{\frac{1}{2}}\|_{L^2}^2$.

Proof. See [17] ∎

If $Id + \hat{h}$ is invertible, we can define:

$$I_{1,1} = I_1 \circ \left(Id + \hat{h}\right)^{-1}. \tag{7}$$

Letting r_1 denote the residual motion such that $I_{1,1} = I_2 \circ (Id + r_1)$, if $Id + \hat{h}$ is ξ-rigid for I_1 then a variable change yields equality $\|(\hat{h} - h^*)|\nabla I_1|^{\frac{1}{2}}\|_{L^2} = \|r_1|\nabla I_{1,1}|^{\frac{1}{2}}\|_{L^2}$, thus giving by Lemma 1 the following bound on the residual motion norm:

$$\|r_1|\nabla I_{1,1}|^{\frac{1}{2}}\|_{L^2} \leq \frac{\pi}{2}\sigma^{d+2}\left(Tr(M_\sigma^{-1})\right)^{\frac{1}{2}} \|h^*|\nabla I_1|^{\frac{1}{2}}\|_{L^2}^2. \tag{8}$$

In view of equality (7) and inequality (8), iterating the motion estimation/registration process looks completely natural and allows for pointing out sufficient conditions for convergence of such a process. Indeed, provided the same assumptions are made at each step, relations (7) and (8) can be seen as recurrence ones, yielding both r_p and $I_{1,p}$ sequences.

4.3 Theoretical iterative scheme

Having control on the residual motion after one registration step, we deduce the following theoretical iterative motion estimation / registration scheme:

1. Initialization: Enter accuracy $\epsilon > 0$ and the maximal number of iterations N. Set $p = 0$, and $I_{1,0} = I_1$.
2. Iterate while $(\|I_{1,p} - I_2\| \geq \epsilon \;\&\; p \leq N)$
   (a) Enter the set of basis functions $\Psi_p = (\psi_{p,i})_{i=1..n_p}$ that linearly and uniquely decompose r_p on the support of $|\nabla I_{1,p}|$.
   (b) Enter scale σ_p and compute: $\hat{h}_p =< \Psi_p, M_{p,\sigma_p}^{-1} B_{\sigma_p} >$.
   (c) Set $I_{1,p+1} = I_{1,p} \circ (Id + \hat{h}_p)^{-1}$.

4.4 Convergence theorem

Now that we have designed an iterative motion estimation / registration scheme, let us infer sufficient conditions for the residual motion to vanish. This leads us to state our following main result:

Theorem 2. *If:*

1. *$\forall p \geq 0$, $I_{1,p} \sim I_2$ (as defined in Section 3.2), and residual motion r_p can be linearly and uniquely decomposed on a set of basis functions $\{\psi_{p,i}, i = 1..n_p\}$;*
2. *$\forall p \geq 0$, there exists a scale $\sigma_p > 0$ such that the set of functions $\{P_{\sigma_p}^{I_{1,p}}(\psi_{p,i}), i = 1..n_p\}$ be free in L^2 and, for $p = 0$, we assume that :*

$$\|h^*|\nabla I_1|^{\frac{1}{2}}\|_{L^2} < \left(\frac{\pi}{2}\sigma_0^{d+2} Tr(M_{0,\sigma_0})^{\frac{1}{2}}\right)^{-1};$$

Set $C_0 = \left(\frac{\pi}{2}\sigma_0^{d+2} Tr(M_{0,\sigma_0})^{\frac{1}{2}} \|h^*|\nabla I_1|^{\frac{1}{2}}\|_{L^2}\right)^{-1}$;

3. *The sequence of conditioning ratios satisfy criteria: $\forall p \geq 0$, $\frac{\sigma_{p+1}^{d+2} Tr(M_{p+1,\sigma_{p+1}})^{\frac{1}{2}}}{\sigma_p^{d+2} Tr(M_{p,\sigma_p})^{\frac{1}{2}}} \leq C_0$;*
4. *$\forall p \geq 0$, estimated deformations $Id + \hat{h}_p \in Hom(D)$ and are ξ-rigid for $I_{1,p}$;*

Then, $\lim_{p\to\infty} \|r_p|\nabla I_{1,p}|^{1/2}\|_{L^2} = 0$.

Proof. See [17] ■

4.5 Numerical algorithm requirements

Firstly, due to the fact that h^* is unknown we have to make an arbitrary choice for the scale at each step. Secondly we at least have to ensure that $Id + \hat{h}$ be invertible at each step. Finally we are faced with the motion basis functions choice.

Multi-scale strategy. The scale choice expresses both a priori knowledge on the motion range and its structure complexity. Here we assume that $(\sigma_p)_p$ is an increasing sequence, starting from $\sigma_0 > 0$ such that:

$$\#S_{\sigma_0} \geq \#\{\text{expected independent motions}\}. \tag{9}$$

Then let $\alpha \in]0, 1[$. In order to justify the minimization problem at new scale $\sigma_{p+1} > \sigma_p$, we will choose it such that:

$$\|(\Pi_{\sigma_{p+1}} - \Pi_{\sigma_p})(I_{1,p+1} - I_2)\|_{L^2} > \alpha \|I_{1,p+1} - I_2\|_{L^2}, \tag{10}$$

Invertibility of $Id + \hat{h}_p$. Let $\beta > 0$. We will apply to $I_{1,p}$ the inverse of the maximal invertible linear part of the computed deformation e.g. $\left(Id + t^*.\hat{h}_p\right)^{-1}$, where

$$t^* = \sup_{t\in[0,1]} \{t \ / \ det(Jac(Id + t.\hat{h}_p)) \geq \beta\}. \tag{11}$$

Choosing the set of basis functions. A major difficulty arising in the theoretical scheme comes from the lack of a priori knowledge on the finite set of basis functions to be entered at each step. In Section 5 we will use an implicit approach via the optimal step gradient algorithm when minimizing the quadratic energy associated to MCE (5).

5 Implicit approach of basis functions and Results

We now use the optimal step gradient algorithm for the minimization of the quadratic functional associated to MCE (5). There are at least two good reasons for doing this:

- the choice of base functions is implicit: it depends on the signals or images I_1 and I_2, and the scale space.
- we can control and stop the quadratic minimization if the associated operator is no longer positive definite.

The general algorithm does not guaranty that the resulting matrix M_{p,σ_p} be invertible. Hence we suggest to systematically use a stopping criteria to control the quadratic minimization, based on the descent speed or simply a maximum number of iterations N_G. In that case our final algorithm writes:

1. Initialization: Enter accuracy $\epsilon > 0$ and the maximal number of iterations N. Set $p = 0$, $I_{1,0} = I_1$, and choose first scale σ_0 according to (9).
2. Iterate while ($\|I_{1,p} - I_2\| \geq \epsilon$ & $p \leq N$ & $\sigma_p \leq 1$)
   (a) Choose σ_p satisfying (10).
   (b) Apply N_G iterations of the optimal step gradient algorithm for the minimization of $E_p(h) = \|\Pi_{\sigma_p}(I_{1,p} - I_2) - P^{I_{1,p}}_{\sigma_p}(h)\|^2_{L^2}$.
   (c) Compute $I_{1,p+1} = I_{1,p} \circ (Id + t^*.\hat{h}_p)^{-1}$ with t^* defined by (11) and increment p.

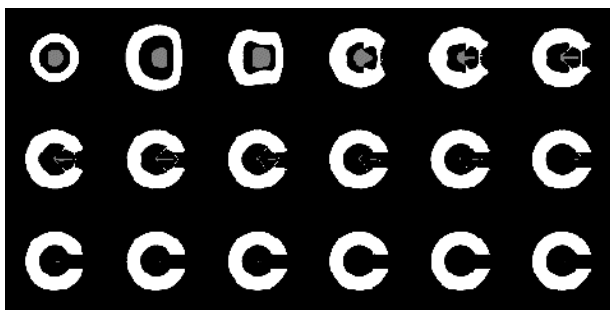

Fig. 4. Registration movie of a target to a 'C' letter. Again, each image corresponds to a step in the iterative scheme.

In the following experiments we have set $\alpha = 2.5\%$, $N_G = 5$, $\beta = 0.1$. In [17], we show results on one-dimensional synthetic and real signals, and with all intensity lines of a stereo pair. Recall that ξ-rigidity is not a constraint when $d = 1$ and thus $\hat{h}_\infty$ is relevant only when $|I_1'(x)| \neq 0$.

We illustrate the algorithm on pairs of images with large deformation for registration applications and movies for motion estimation applications.

Registration problems involving large deformation: In figure 4 we show the different steps of the algorithm performing the registration between the first and last images. In Figure 5, we show the study and target images, and the

Fig. 5. Scene registration example: Study image (left), deformed Study image onto Target image (center), and Target image (right).

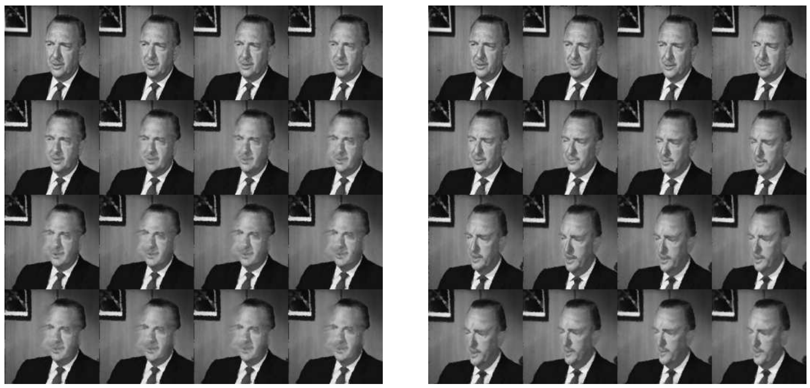

Fig. 6. On the left, registered sequence of the original sequence onto first image using the computed backward motions. On the right, movie obtained by deforming only the first image of Cronkite movie using the sequence of computed motions

deformed study image after applying the estimated motion.
Optical Flow estimation examples: in Figure 6 we show the sequence of the registered images of the original Cronkite sequence onto first image using the sequence of computed backward motions. The result is expected to be motionless. On top of Figure 6, we show the complete movie obtained by deforming iteratively only the first image of Cronkite movie. For that we use the sequence of computed motions between each pair of consecutive images of the original movie. In Figure 6 on the bottom, we see the error images.

6 Conclusion

We have addressed the theoretical problems of motion estimation and registration of signals or images in any dimension. We have used the main features of previous works on the subject to formalize them in a framework allowing a rigorous mathematical analysis. More specifically we wrote a new ridigity hypothesis that we used to infer a unique Motion Constraint Equation with small remainder at coarse scales. We then showed that upon hypotheses on the motion norm and structure/scale tradeoff, an iterative motion estimation/registration scheme could converge towards the expected solution of the problem e.g. the global minimum of the nonlinear least square problem energy. Since each step of the theoretical scheme needs a set of motion basis functions which are not known, we have designed an implicit algorithm and illustrated the method in dimension one and two, including large deformation examples.

References

1. L. Alvarez, J. Esclarin, M. Lefébure, J. Sanchez. A PDE model for computing the optical flow. *Proc. XVI Congresso de Ecuaciones Diferenciales y Aplicaciones*, Las Palmas, pp. 1349–1356, 1999.
2. L. Alvarez, J. Weickert, J. Sanchez, Reliable estimation of dense optical flow fields with large displacements. TR 2, Universidad de Las Palmas, November 1999.
3. G. Aubert, R. Deriche and P. Kornprobst. Computing optical flow via variational techniques. *SIAM J. Appl. Math.*, Vol. 60 (1), pp. 156–182, 1999.
4. N. Ayache. Medical computer vision, virtual reality and robotics. IVC (13), No 4, May 1995, pp 295-313.
5. Ruzena Bajcsy and Stane Kovacic. Multiresolution elastic matching. CVGIP, (46), No 1, pp. 1–21, 1989.
6. J.L. Barron, D.J. Fleet, and S.S. Beauchemin. Performance of optical flow. IJCV, 12(1):43–77, 1994.
7. M. Ben-Ezra, B. Rousso, and S. Peleg. Motion segmentation using convergence properties. In *ARPA Im. Unders. Workshop*, pp II 1233-1235, 1994.
8. J.R. Bergen and E.H. Adelson. Hierarchical, computationally efficient motion estimation algorithm. *J. of the Optical Society Am.*, 4(35), 1987.
9. P. Bouthemy and J.M. Odobez. Robust multiresolution estimation of parametric motion models. *J. of Vis. Comm. and Image Repres.*, 6(4):348–365, 1995.
10. G. Christensen, R.D. Rabbitt, and M.I. Miller. 3D brain mapping using a deformable neuroanatomy. *Physics in Med and Biol*, (39), March :609–618, 1994.
11. D. Fleet, M. Black, Y. Yacoob and A. Jepson. Design and use of linear models for image motion analysis. *IJCV*, 36(3), 2000.
12. P.R. Giaccone, D. Greenhill, G.A. Jones. Recovering very large visual motion fields. *SCIA97*, pp 917-922.
13. B.K.P. Horn and Brian Schunck. Determining optical flow. *Artificial Intelligence*, (17) (1-3) :185–204, 1981.
14. M. Irani, B. Rousso, and S. Peleg. Detecting and tracking multiple moving objects using temporal integration. In *ECCV92*, pp 282–287, 1992.
15. M. Lefébure Estimation de Mouvement et Recalage de Signaux et d'Images: Formalisation et Analyse. PhD Thesis, Université Paris-Dauphine, 1998.
16. Martin Lefébure and Laurent D. Cohen. A multiresolution algorithm for signal and image registration. In *In Proc. ICIP'97*, Santa Barbara, California, Oct. 1997.
17. M. Lefébure and L. D. Cohen. Motion estimation and registration of signals and images: formalization and analysis. CEREMADE Technical Report, 0102, January 2001. To appear in Journal of Mathematical Imaging and Vision.
18. D. Terzopoulos. Multiresolution algorithms in computational vision. *Image Understanding*. S. Ullman, W. Richards, 1986.
19. J.P. Thirion. Fast non-rigid matching of 3D medical images. TR 2547, INRIA, 1995.
20. A. Trouvé. Diffeomorphisms groups and pattern matching in image analysis. IJCV, 28(3), 1998.
21. J. Weickert. On discontinuity-preserving optic flow. *Proc. Computer Vision and Mobile Robotics Workshop*, Santorini, pp. 115–122, Sept. 1998.
22. G. Whitten. A framework for adaptive scale space tracking solutions to problems in computational vision. In *ICCV'90, Osaka*, pp 210–220, Dec 1990.
23. A. Witkin, D. Terzopoulos, M. Kass. Signal matching through scale space. IJCV, 1(2):133–144, 1987.